Reactive Flux Calculations of Methyl Vinyl Ketone Reacting with Cyclopentadiene in Water

Youngshang Pak and Gregory A. Voth*

Department of Chemistry and Henry Eyring Center for Theoretical Chemistry, University of Utah, Salt Lake City, Utah 84112

Received: September 18, 1998; In Final Form: December 4, 1998

Molecular dynamics and reactive flux simulations of the Diels−Alder reaction of methyl vinyl ketone (MVK) reacting with cyclopentadiene (CPD) in water have been carried out to calculate the activation free energy and transmission coefficient for the reaction. For this purpose, an empirical potential energy surface (PES) of the reaction was developed by first constructing an intramolecular PES of MVK + CPD using the B3LYP/6-31+g* level of ab initio theory. This calculation predicts that the reaction barrier height of MVK + CPD in the gas phase is 16 kcal/mol. The MVK + CPD complex was then surrounded by 215 SPC/F2 water molecules, and the activation free energy is seen to be reduced by 2.2 kcal/mol compared to that of the gas phase. The initial conditions for the reactive flux calculations were obtained at $T = 300$ K by a Nosé-Hoover chain dynamics algorithm that was recently developed for this purpose. These calculations show that the transmission coefficient for the reaction in water is 0.67 and therefore that the dominant solvent effect is the static reduction in the activation free energy barrier.

I. Introduction

It has been known experimentally that the Diels−Alder reaction of methyl vinyl ketone (MVK) with cyclopentadiene (CPD) is significantly accelerated in aqueous solvents.[1,2] Jorgensen et al.[3,4] have carried out Monte Carlo calculations to study solvent effects on the reaction and suggested that the aqueous rate enhancement is due to hydrogen bonding between the solute and water molecules in the transition state. Other models such as continuum solvent approaches have also been employed[5,6] to investigate the rate acceleration of Diels−Alder reactions in the presence of water. However, in all the theoretical models employed so far, dynamic solvent effects on the rate of the MVK + CPD reaction have also not been taken into account, so the dominant role of the solvent could not be conclusively elaborated. The dynamical (transition recrossing) effect can be incoporated in terms of a transmission coefficient by reactive flux (RF) calculations.[7] The main purpose of the present work is to therefore calculate the activation free energy for the reaction in water and then, on the same footing, to calculate the dynamical transmission coefficient to distinguish between the two possible solvent effects for the reaction of MVK + CPD.

In our approach, an empirical intramolecular potential energy surface (PES) for MVK + CPD was developed using gas phase ab initio data at the B3LYP/6-31+g* level. This was accomplished by identifying an appropriate reaction coordinate involved in the reaction. This approach is quite similar to a method for constructing a reactive PES, which has been applied to proton-transfer reactions of polyatomic molecules such as malonaldehyde and $H_5O_2^+$.[8] The interactions between the solute species and the water solvent (or between the water molecules themselves) are then included via partial charges and Lennard-Jones (LJ) potentials. Instead of using a fixed charge model for the solute, its partial charges are allowed to change along the reaction coordinate in order to reproduce the results of the ab initio calculations. The free energy of solvation for the reaction of MVK + CPD was then obtained by the potential of mean force (PMF) calculations for both the gas phase and water solvent environment and compared to other previously published results and to experiment.

To perform the RF calculations, initial conditions constrained at a plane dividing the reactant and product regions must be generated according to the flux-weighted canonical distribution.[9] Recently, Jang and Voth[10] have proposed simple reversible molecular dynamics (MD) algorithms based on Nosé-Hoover chain (NHC) dynamics and successfully tested them for a model system of coupled harmonic oscillators. The algorithms can easily be extended to systems with holonomic constraints, which is required in the sampling procedure for the RF initial conditions. Using the NHC dynamics method, the RF initial conditions for the MVK + CPD complex in water were generated, from which independent RF trajectores were obtained to statistically average the reactive flux correlation function.

The sections of this paper are organized as follows: In section II the method for constructing the intramolecular potential is described. Then, in section III the potential of mean force calculation in water is presented, while section IV describes the reactive flux results. Section V contains concluding remarks.

II. Intramolecular Potential Energy Surface of Methyl Vinyl Ketone (MVK) and Cyclopetadiene (CPD)

Let us define q_i ($i = 1, ..., 3N - 6$) to be the curvilinear internal coordinates of a reactive species consisting of N atoms. Then, introducing a reaction coordinate ξ that is mainly responsible for a large amplitude motion during the reaction leads to a partition of the $3N - 6$ internal coordinates into the reaction coordinate ξ and the remaining spectator ones r_i ($i = 1, ..., 3N - 7$). The intramolecular potential energy surface of the reactive species can next be expressed as

$$V_{\text{solute}}^{\text{intra}}(\mathbf{r},\xi) = V_0(\xi) + \frac{1}{2}\sum_{i,j}^{3N-7} F_{i,j}(\xi)[r_i - u_i(\xi)][r_j - u_j(\xi)] \tag{1}$$

where $V_0(\xi)$ is the minimum energy at ξ and $F_{i,j}(\xi)$ are the

10.1021/jp983785s CCC: $18.00
Published on Web 01/23/1999

elements of the reduced Hessian matrix consisting of the spectator variables defined at ξ. In eq 1, $u_i(\xi)$ ($i = 1, ..., 3N - 7$) represent the internal coordinates of the spectator variables corresponding to the minimum energy path along ξ, obeying

$$\frac{\partial V_{\text{solute}}^{\text{intra}}(\mathbf{r},\xi)}{\partial \mathbf{r}} = 0 \tag{2}$$

For the internal displacement coordinates involving dihedral angles, $r_i - u_i(\xi)$ is replaced with $\sin[r_i - u_i(\xi)]$ to impose periodicity.

In the current system of MVK + CPD ($N = 22$), one might in fact choose 2-dimensional (2D) reaction coordinates by selecting the two forming (or breaking) C−C bond distances of MVK + CPD, since they obviously exhibit large amplitude motions during the reaction process. Even though this choice provides a more flexible and accurate description for PES, it leads to quite a large number of 2D grid calculations, which is not yet practical for state-of-the-art ab initio methods with the current system size. Therefore, to make the construction of the PES more feasible in this case, we have chosen ξ to be one of the two C−C bonds, so that the other C−C bond becomes a dependent variable on ξ. The potential energy surface expression with the one reaction coordinate in eq 1 still requires extensive computations of $V_0(\xi)$, $u_i(\xi)$ ($i = 1, ..., 3N - 7$), and $F_{i,j}(\xi)$ ($i, j = 1, ..., 3N - 7$).

The Hessian matrix calculations for a wide range of ξ to cover the overall reaction process are computationally demanding. Thus we attempted to introduce more approximate Hessian matrices for the intermediate regions not including reactants, transition state (TS), and product, by calculating the individiual matrix elements only for those three states and then connecting them smoothly using an empirical switching function. For this purpose, the following switching function was employed:

From TS to reactant:

$$f^{\text{r}}(\xi) = [(\xi_{2,\text{r}}{}^2 - \xi^2)^2 + 2\xi^2 - 3\xi_{1,\text{r}}{}^2]/(\xi_{2,\text{r}}{}^2 - \xi_{1,\text{r}}{}^2)^3, \quad \xi_{1,\text{r}} \le \xi \le \xi_{2,\text{r}}$$
$$= 1, \xi < \xi_{1,\text{r}}$$
$$= 0, \xi > \xi_{2,\text{r}} \tag{3}$$

From TS to product:

$$f^{\text{p}}(\xi) = [(\xi_{1,\text{p}}{}^2 - \xi^2)^2 + 2\xi^2 - 3\xi_{2,\text{p}}{}^2]/(\xi_{1,\text{p}}{}^2 - \xi_{2,\text{p}}{}^2)^3, \quad \xi_{1,\text{p}} \le \xi \le \xi_{2,\text{p}}$$
$$= 1, \xi > \xi_{2,\text{p}}$$
$$= 0, \xi < \xi_{1,\text{p}} \tag{4}$$

where $\xi_{1,\text{r(p)}}$ and $\xi_{2,\text{r(p)}}$ are the cutoff variables for the interpolation from the transition state to the reactants (product). The polynomial functions of ξ in eqs 3 and 4 are designed to make a smooth transition from 0 to 1. With $F_{i,j}^{\text{r}}(\xi)$, $F_{i,j}^{\text{t}}(\xi)$, and $F_{i,j}^{\text{p}}(\xi)$ ($i, j = 1, ..., 3N - 7$) denoted to be the reduced Hessian matrix elements for the reactants, the transition state, and the product, respectively, the matrix elements at ξ can be computed by using

$$F_{i,j}(\xi) = F_{i,j}^{t} f^{\text{r}}(\xi) + F_{i,j}^{\text{r}}[1 - f^{\text{r}}(\xi)] \qquad \text{from TS to reactants} \tag{5}$$

$$F_{i,j}(\xi) = F_{i,j}^{t} f^{\text{p}}(\xi) + F_{i,j}^{\text{p}}[1 - f^{\text{p}}(\xi)] \qquad \text{from TS to product} \tag{6}$$

As a consequence, the expressions in eqs 5 and 6 reproduce correct ab initio Hessian matrix elements at each of the three states, although they are interpolated in an approximate manner for the intermediate regions. The main advantage of using eqs 5 and 6 is that one can avoid calculating all the possible Hessian matrices by using the ab initio method and fitting their individual elements [in this case the total number of Hessian matrix elements to be fitted is $(N - 1)N/2 = 1770$]. Recently, Minichino and Voth[8] derived a general analytic expression for the Hessian matrices for spectator variables based on the minimum coupling approximation. Their method could be used as an alternative way to obtain the Hessian matrix elements.

Figure 1. The B3LYP/6-31+g* transition state structure of MVK + CPD. The reaction coordinate ξ chosen in this work is indicated by a white bond.

To find $V_0(\xi)$ and $u_i(\xi)$, restricted geometry optimizations were carried out for 1.09 Å $\le \xi \le$ 10.0 Å at the B3LYP/6-31+g* level of theory, using the GAUSSIAN 94 quantum chemistry program,[11] and the Hessian matrices were obtained for the three states. The computed transition state geometry is shown in Figure 1, and the reaction coordinate chosen in this work is indicated by a white line. For convenience, $u_i(\xi)$ for the reactant state were calculated by the optimization at $\xi =$ 10.0 Å. A total of 25 frames along ξ were computed, and the resulting $V_0(\xi)$ and $u_i(\xi)$ were interpolated by the cubic spline fit method.[12] The optimized structures of MVK + CPD at $\xi =$ 3.1, 2.0, and 1.6 Å are shown in Figure 2 from left to right, respectively, to demonstrate the structural changes of MVK + CPD during the reaction. Note that for trajectory calculations the gradients of the spline fitted variables can be easily obtained by directly differentiating the spline functionals.

The fitted minimum energy function, $V_0(\xi)$, is given in Figure 3, indicating that the transition state occurs at $\xi \sim 2.0$ Å and that the gas-phase barrier height from the reactants to transition state is 16.3 kcal/mol. The ab initio barrier heights were also calculated at the MP2, MP4, and CCSD(T) levels, using the B3LYP/6-31+g* optimized geometries, to investigate more details of the energetics for the MVK + CPD reaction. As can be seen in Table 1, surprisingly the MP2 barrier is only 3.4 kcal/mol, but both the MP4SDQ and CCSD results agree well with the B3LYP value. The triple substitution effects in the coupled cluster method, however, decreases the barrier height by 4 kcal/mol, but it should be noted that the geometries were not optimized at this level of theory due to the computational cost involved (the B3LYP geometries where used). Such a geometry optimization might lead to better agreement between the B3LYP and CCSD(T) results. It is also interesting to note

Figure 2. The B3LYP/6-31+g* optimized structures at $\xi = 3.1$, 1.9948, and 1.5948 Å from left to right, respectively. The structure in the middle corresponds to the transition state geometry.

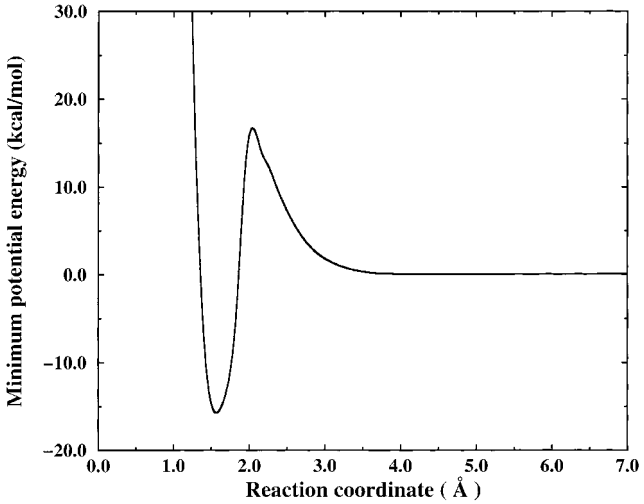

Figure 3. 1D minimum energy surface along the reaction coordinate ξ calculated by B3LYP/6-31+g*. The barrier heights are 16.3 kcal/mol from the reactant to the transition state and 32.2 kcal/mol from the product to the transition state. The barrier heights are calculated without zero-point vibrational energy corrections.

TABLE 1: Ab Initio Energy Barriers for the Reaction of MVK + CPD in the Gas Phase, Using the 6-31+g* Basis Set

method	CPD (au)	MVK (au)	TS (au)	$\Delta E^{\ddagger}$ (kcal/mol)
BLYP[a]	−194.008 380	−231.155 645	−452.139 979	15.1
B3LYP[a]	−194.110 328	−231.247 285	−425.331 638	16.3
MP2[b]	−193.437 312	−230.501 802	−423.933 727	3.4
MP4SDQ[b]	−193.476 373	−230.542 106	−423.990 341	17.7
MP4[b]	−193.505 329	−230.570 428	−424.062 266	8.5
CCSD[b]	−193.477 280	−230.541 105	−423.989 773	18.0
CCSD(T)[b]	−193.506 150	−230.568 326	−424.005 251	12.1

[a] The values were obtained at the optimized geometries for the methods indicated. [b] The values were calculated using the B3LYP/6-31+g* optimized geometries.

that the BLYP barrier is very close to the B3LYP one for this reaction. The cutoff variables in eqs 3 and 4 were chosen to be $\xi_{1,p} = 1.75$ Å, $\xi_{2,p} = 1.94$ Å, $\xi_{1,r} = 2.23$ Å, and $\xi_{2,r} = 7.0$ Å.

Nonbonded interactions between the atomic sites on the complex and the solvent water molecules (or between water molecules) consisted of Lennard-Jones (LJ) and Coulomb interactions:

$$V_{i,j}^{\text{inter}} = \frac{1}{4\pi\epsilon_0}\frac{q_i q_j}{r_{ij}} + 4\epsilon_{i,j}\left[\left(\frac{\sigma_{i,j}}{r_{ij}}\right)^{12} - \left(\frac{\sigma_{i,j}}{r_{ij}}\right)^{6}\right] \qquad (7)$$

TABLE 2: Partial Charges of the Carbonyl Group (C═O) of MVK + CPD in the Product, the Transition State (TS), and the Reactants, Calculated by Using the RESP Method at the B3LYP/6-31+g* Level of Theory[a]

	reactants	TS	product
q(C)	0.73 (0.53)	0.71 (0.56)	0.64 (0.55)
q(O)	−0.54 (−0.56)	−0.57 (−0.61)	−0.53 (−0.54)

[a] The values in parentheses are ones obtained by the Mulliken charge analysis at the HF/6−31 g(d) level (ref 3).

where $\epsilon_{i,j}$ and $\sigma_{i,j}$ are the LJ parameters and q_i are the partial charges on ith atom. The values of Cornell et al.[13] were used for the LJ type interactions with an additional scaling of a factor 1.12 of the σ values, and Ewald summation was used to treat the long-range Coulomb interactions for the solute−water and water−water molecules. For water molecules, the SPC/F2 parameters[14] were employed.

It is also important to take into account the effects of atomic charge variations in the reactive species as the reaction proceeds. In a manner similar to the Hessian matrix interpolation, a dynamic model for the solute charges was implemented by calculating the atomic charges of the three states and interpolating them using eqs 3 and 4. In this case, the same cutoff variables as in the Hessian matrix were used, except for $\xi_{2,r} = 3.1$ Å, beyond which the variation in the atomic charges of the solute was insignificant. With this procedure the atomic charges of the solute $\{q_i(\xi); i = 1, N\}$ were thus parametrized to depend on only the reaction coordinate ξ. The atomic charges of the solute were computed by the restrained electrostatic potential (RESP) method[15] at the B3LYP/6-31+g* level. The partial charges on the carbonyl group (C═O) in the MVK + CPD complex are given in Table 2, while the other parameters are available upon request. Our results indicate that the polarization of the carbonyl bond at the transition state may be somewhat larger than in the previous Mulliken analysis at the Hartree−Fock (HF) level.[3] The previously calculated oxygen partial charges are quite comparable to the current values, but the carbon partial charges are consistently smaller than our values (cf. Table 2).

III. Potential of Mean Force and Free Energy Barrier of MVK + CPD in Water

To investigate static solvent effects on the reaction of MVK + CPD in water, PMF calculations were carried out for the reacting species. With the current choice of ξ, the mean force $f(\xi)$ is simply obtained by

$$f(\xi) = -\left\langle \frac{\partial V}{\partial \xi} - \frac{2k_B T}{\xi} \right\rangle_{\xi} \tag{8}$$

where $\langle ... \rangle_{\xi}$ denotes the average over the restricted ensemble $\xi = \xi_0$. The potential of mean force $W(\xi)$ was then calculated by integrating $f(\xi)$:

$$W(\xi) = W(\xi_{\text{ref}}) - \int_{\xi_{\text{ref}}}^{\xi} \mathrm{d}\xi'\, f(\xi') \tag{9}$$

where ξ_{ref} is a reference point for the integration.

In our simulations, we averaged over the constrained ensemble $\xi = \xi_0$ and $\dot{\xi} = 0$. This bias, however, can be removed by introducing a weighting factor, such that

$$\langle A \rangle_{\xi} = \frac{\langle Z_{\xi}^{-1/2} A \rangle_{\text{c}}}{\langle Z_{\xi}^{-1/2} \rangle_{\text{c}}} \tag{10}$$

where $\langle ... \rangle_{\text{c}}$ is the average over the constrained ensemble and Z_{ξ} is defined by

$$Z_{\xi} = \sum_{i=1}^{N} \frac{1}{m_i} \frac{\partial \xi}{\partial \mathbf{x}_i} \cdot \frac{\partial \xi}{\partial \mathbf{x}_i} \tag{11}$$

with m_i and $\boldsymbol{x}_i$ being the mass and Cartesian coordinates of ith atom for the solute, respectively. For this definition of ξ, Z_{ξ} is a diagonal component of the **G** matrix corresponding to $\xi = r$, i.e., $\boldsymbol{G}_{\xi\xi}$, which is just a reduced mass $m_i^{-1} + m_j^{-1}$. As a result, $\langle \mathrm{A} \rangle_{\xi}$ equals $\langle \mathrm{A} \rangle_{\text{c}}$. The probability distribution for the constained ensemble $\xi = \xi_0$ and $\dot{\xi} = 0$ is given by

$$P_{\xi}^{\text{c}}(\Gamma)\, \mathbf{d}\Gamma \equiv \frac{\mathbf{d}\Gamma\, \delta(\xi - \xi_0)\, \delta(\dot{\xi}) \exp(-\beta H)}{\int \mathbf{d}\Gamma\, \delta(\xi - \xi_0)\, \delta(\dot{\xi}) \exp(-\beta H)} \tag{12}$$

Recently, Jang and Voth[10] proposed several reversible MD algorithms based on Nosé-Hoover chains to generate trajectories according to canonical distributions. In the present work their velocity Verlet algorithm (VV-1)[10] was employed to generate the initial conditions according to $P_{\xi}^{\text{c}}(\Gamma)$ in eq 12. For more details of the algorithm, the reader should refer to ref 9.

The total MD system consisted of the MVK + CPD complex and 215 SPC/F2 water molecules in a cubic box of side length 19.5 Å. A total of 41 frames along ξ (1.3 Å $\leq \xi \leq$ 7.5 Å) were equilibrated for 20 ps, and the corresponding PMF values were sampled for 25−50 ps. A time step of 0.25 fs was used in the trajectory integration. The resulting PMF curves of MVK + CPD in both the gas and aqueous phases are shown in Figure 4. For comparison, in the Monte Carlo simulation of Jorgensen et al.,[3,4] only free energies of solvation were computed along the reaction path, using a rigid model of both solute and solvent.

As seen in Figure 4, including the molecular vibrations in the solute leads to substantial changes in the free energy barrier, even in the gas phase. The gas-phase minimum energy barriers at the B3LYP/6-31+g* level are 32 kcal/mol (from the product to TS) and 16 kcal/mol (from the reactants to TS), but our PMF calculations show that the corresponding free energy barriers are 16.4 ± 0.1 kcal/mol and 11.7 ± 0.9 kcal/mol, respectively. The deviations mostly result from thermal excitations of vibrational modes of the reaction complex.

The reactive free energy barrier of MVK + CPD in water is calculated to be 9.5 ± 1.0 kcal/mol, which is smaller than the gas-phase value by 2.2 kcal/mol. This value is less than the result derived from the experimental data (3.8 kcal/mol)[1,2] and the theorectical value of Jorgensen et al. (4.2 kcal/mol).[3,4] The experimental value, however, is reasonably close to our calculated value. It is possible that the underestimation of the solvation free energy in the present work is due to lack of polarizability of the solute model potential constructed from the gas-phase B3LYP data, as well as solvent polarizability effects. The solute polarization effects might be estimated by using continuum models of the solvent in the framework of ab initio methods, but these estimates can be ill-defined for such a complex system. Further improvement could be anticipated if the SPC/F2 water potential were replaced by a flexible, polarizable one. Such a model, which accurately reproduces the properties of water, does not yet appear to exist.

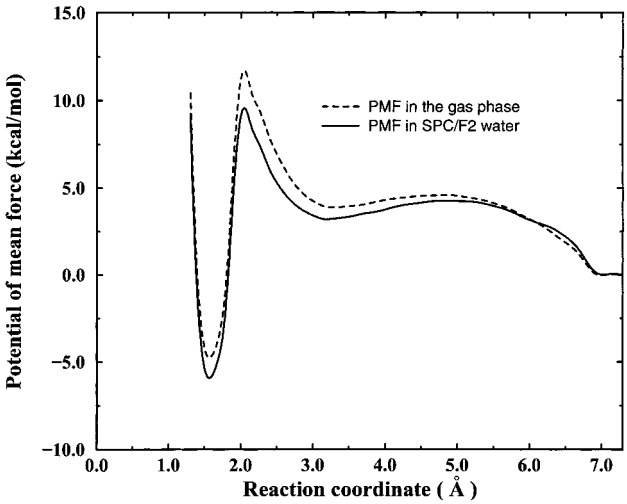

Figure 4. Potentials of mean force [$W(\xi)$] of the MVK + CPD reaction in the gas phase and water environment at $T = 300$ K. The dashed and solid lines denote the PMFs in the gas and water phases, respectively.

IV. Reactive Flux Calculations of MVK + CPD in Water

In reactive flux calculations, the dynamic transmission coefficient κ, which corrects the transition state (TST) rate constant k^{TST}, can be calculated by virtue of the formula

$$\kappa \equiv \frac{k}{k^{\text{TST}}} = \langle \theta_{\text{p}}[\xi(t_{\text{pl}})] \rangle_{+} - \langle \theta_{\text{p}}[\xi(t_{\text{pl}})] \rangle_{-} \tag{13}$$

where k is the true rate constant, $\xi(t_{\text{pl}})$ is the reaction coordinate at plateau times t_{pl}, and θ_p is a step function, such that θ_p is unity only if $\xi(t_{\text{pl}})$ is in the product region and zero otherwise. The notations $\langle ... \rangle_{+}$ and $\langle ... \rangle_{-}$ in eq 13 denote averaging over a normalized flux weighted canonical distribution function with positive and negative initial reaction coordinate velocities, respectively. The normalized flux weighted distribution function at $\Gamma \equiv (\mathbf{x}, \mathbf{p}^{\mathbf{x}})$ in Cartesian coordinates is given by[9]

$$P^{(\pm)}(\Gamma)\, \mathbf{d}\Gamma = \frac{\mathbf{d}\Gamma\, \delta[\xi(0) - \xi^{\ddagger}] \theta_{\text{p}}[\pm\dot{\xi}(0)] |\dot{\xi}(0)| \exp(-\beta H)}{\int \mathbf{d}\Gamma\, \delta[\xi(0) - \xi^{\ddagger}] \theta_{\text{p}}[\pm\dot{\xi}(0)] |\dot{\xi}(0)| \exp(-\beta H)} \tag{14}$$

where $\xi^{\ddagger}$ is a plane dividing the reactant and product regions of a reactive system consisting of N atoms, and $\xi(0)$ and $\dot{\xi}(0)$ are the reaction coordinate and velocity, respectively, at the initial time $t = 0$. In this work, bond length constraints have not been employed.

The flux weighted distribution in eq 13 can also be rewritten as

$$P^{(\pm)}(\Gamma)\,\mathbf{d}\Gamma = \Big[\mathbf{d}\Gamma\,\delta(\xi-\dot{\xi}^{\ddagger})\,\delta(\dot{\xi})\exp(-\beta H)\,\mathrm{d}\dot{\xi}'\times |\dot{\xi}'|\theta_{\mathrm{p}}(\pm\dot{\xi}')\exp\Big(-\frac{1}{2}\beta\dot{\xi}'Z_{\xi}^{-1}\dot{\xi}'\Big)\Big]\Big/\Big[\int \mathbf{d}\Gamma\,\delta(\xi-\xi^{\ddagger})\,\delta(\dot{\xi})\times \exp(-\beta H)\int_0^{\infty}\mathrm{d}\dot{\xi}'\,|\dot{\xi}'|\theta_{\mathrm{p}}(\pm\dot{\xi}')\exp\Big(-\frac{1}{2}\beta\dot{\xi}'Z_{\xi}^{-1}\dot{\xi}'\Big)\Big] \quad (15)$$

The average value of the step function $\theta_p[\xi(t)]$ sampled by the distribution in eq 15 exactly reproduces that of eq 14, and a proof is given in the Appendix. The flux averages in eq 13 can be expressed in more practical terms as

$$\langle\theta_{\mathrm{p}}[\xi(t_{\mathrm{pl}})]\rangle_{\pm} = \frac{\int \mathbf{d}\Gamma\,P^{\mathrm{c}}_{\xi}(\Gamma)\int_0^{\infty}\mathrm{d}\dot{\xi}'\,P^{(\pm)}(\dot{\xi}'|\mathbf{x})Z_{\xi}\theta_{\mathrm{p}}[\xi(t_{\mathrm{pl}})]}{\int \mathbf{d}\Gamma\,P^{\mathrm{c}}_{\xi}(\Gamma)Z_{\xi}} \quad (16)$$

with

$$P^{(\pm)}(\dot{\xi}'|\mathbf{x})\,\mathrm{d}\dot{\xi}' \equiv \frac{\mathrm{d}\dot{\xi}'\,|\dot{\xi}'|\theta_{\mathrm{p}}(\pm\dot{\xi}')\exp\Big(-\frac{1}{2}\beta\dot{\xi}'Z_{\xi}^{-1}\dot{\xi}'\Big)}{\int_0^{\infty}\mathrm{d}\dot{\xi}'|\dot{\xi}'|\theta_{\mathrm{p}}(\pm\dot{\xi}')\exp\Big(-\frac{1}{2}\beta\dot{\xi}'Z_{\xi}^{-1}\dot{\xi}'\Big)} \quad (17)$$

where $P^{(\pm)}(\dot{\xi}'|\mathbf{x})$ is the conditional probability of the reaction velocity $\dot{\xi}'$ for a given value of $\mathbf{x}$. [The superscripts (+) and (−) represent the forward and backward reaction velocities, respectively.] For the sampling of a negative $\dot{\xi}'$, it can easily be generated by using $P^{(+)}(\dot{\xi}'|\mathbf{x})$ and just reversing the sign without resampling $P^{(-)}(\dot{\xi}'|\mathbf{x})$. The canonical MD algorithm in ref 9 was used to generate the distribution of $P^{\mathrm{c}}_{\xi}(\Gamma)$ in eq 12. Thus, after the canonical equilibrium of $P^{\mathrm{c}}_{\xi}(\Gamma)$ is reached, one has to assign only the value of $\dot{\xi}$, simply using $P^{(\pm)}(\dot{\xi}'|\mathbf{x})$ in eq 17.

The analytic expression of Z_ξ in eq 11 depends on the choice of the dividing plane. Using a Cartesian coordinate expression, Otter and Briels[16] have introduced an unstable normal mode Q_1 (i.e., a normal mode having a negative eigenvalue at a transition state) for the definition of the plane in their RF calculations. Often it is convenient to express normal modes in $3N-6$ curvilinear internal coordinates:

$$Q_i = \sum_{j=1}^{3N-6} L_{i,j}^{-1}(S_j - S_{\mathrm{e},j}) \quad (18)$$

where $L_{i,j}^{-1}$ are the elements of the transformation matrix from the internal coordinates $\{S_j\}$ to the normal coordinates $\{Q_i\}$ and $\{S_{\mathrm{e},j}\}$ are the internal coordinates at the transition state. If the unstable normal mode Q_1 is used for the definition of ξ, substituting $\xi = Q_1$ into eq 11 and using eq 18 gives

$$Z_{\xi} = \sum_{j=1}^{3N\text{-}6}\sum_{k=1}^{3N-6} L_{1,j}^{-1}L_{1,k}^{-1}\sum_{i=1}^{3N} B_{j,i}\,m_i^{-1}B_{i,k}^{\mathrm{T}} = \sum_{j=1}^{3N\text{-}6}\sum_{k=1}^{3N\text{-}6} L_{1,j}^{-1}G_{j,k}(L^{-1})_{k,1}^{\mathrm{T}} = [\mathbf{L}^{-1}\cdot\mathbf{G}\cdot(\mathbf{L}^{-1})^{\mathrm{T}}]_{1,1} \quad (19)$$

where $B_{j,k}$ are the elements of the $\mathbf{B}$ matrix, and the $\mathbf{G}$ matrix is defined to be $\mathbf{G} \equiv \mathbf{B}\cdot\mathbf{M}^{-1}\cdot\mathbf{B}^{\mathrm{T}}$.[17] In general the $\mathbf{G}$ matrix at an instantaneous position can be written as

$$\mathbf{G} = \mathbf{G}_0 + \Delta\mathbf{G} \quad (20)$$

where $\mathbf{G}_0$ is the matrix evaluated at the transition state and $\Delta\mathbf{G}$ is the remaining term depending on the deviation from it. Then Z_ξ can be rewritten as

$$Z_{\xi} = [\mathbf{L}^{-1}\cdot\mathbf{G}_0\cdot(\mathbf{L}^{-1})^{\mathrm{T}}]_{1,1} + [\mathbf{L}^{-1}\cdot\Delta\mathbf{G}\cdot(\mathbf{L}^{-1})^{\mathrm{T}}]_{1,1} = 1 + \Delta Z_{\xi} \quad (21)$$

The first term in eq 21 is unity, since $\mathbf{L}^{\mathrm{T}}\cdot\mathbf{G}_0^{-1}\cdot\mathbf{L} = \mathbf{I}$ by the definition of the $\mathbf{L}$ matrix.[18] The value of Z_ξ begins to deviate from unity, depending on the magnitude of ΔZ_ξ, as the molecular complex moves away from the transition state, which has also been pointed out by Otter and Briels.[16] The choice of the dividing plane as the unstable normal mode is particularly useful in the case that many degrees of freedom contribute to defining a reaction coordinate of a system. This definition can also provide a natural choice of the RF plane for reactive systems whose PES are parametrized by the intrinsic reaction coordinate (IRC),[19] since $\xi = Q_1$ is closely related to the IRC.

In the current case, however, one can choose a simple bond distance for the reaction coordinate (i.e., $\xi = r$). In this case, noting that $Z_\xi = \mathbf{G}_{\xi\xi} = m_i^{-1} + m_j^{-1}$, the expression in eq 16 is simplified to

$$\langle\theta_{\mathrm{p}}[\xi(t_{\mathrm{pl}})]\rangle_{\pm} = \int \mathbf{d}\Gamma\,P^{\mathrm{c}}_{\xi}(\Gamma)\int_0^{\infty}\mathrm{d}\dot{\xi}'\,P^{(\pm)}(\dot{\xi}'|\mathbf{x})\theta_{\mathrm{p}}[\xi(t_{\mathrm{pl}})] \quad (22)$$

Then the transmission coefficient in eq 13 is calculated by

$$\kappa = \int \mathbf{d}\Gamma\,P^{\mathrm{c}}_{\xi}(\Gamma)\int_0^{\infty}\mathrm{d}\dot{\xi}'\,[P^{(+)}(\dot{\xi}'|\mathbf{x})\theta_{\mathrm{p}}[\xi(t_{\mathrm{pl}})] - P^{(-)}(\dot{\xi}'|\mathbf{x})\theta_{\mathrm{p}}[\xi(t_{\mathrm{pl}})]] \quad (23)$$

After $\dot{\xi}$ is sampled using $P^{(\pm)}(\dot{\xi}'|\mathbf{x})$, it should be transformed into the corresponding Cartesian velocities. According to Otter and Briel's approach,[16] the Cartesian velocity of the ith atom contributing from only $\dot{\xi}$ can be obtained by

$$\mathbf{v}_i = \mathbf{M}_i^{-1/2}\cdot\mathbf{f}\cdot\sum_{j=1}^{3N-6}\mathbf{l}_{i,j}\dot{Q}_j = \mathbf{M}_i^{-1/2}\cdot\mathbf{f}\cdot\sum_{j=1}^{3N-6}\mathbf{l}_{i,j}L_{j,k(\xi)}^{-1}\dot{\xi} \quad (24)$$

where the subscript $k(\xi)$ in the $\mathbf{L}^{-1}$ matrix denotes the internal coordinate variable corresponding to ξ, and $\mathbf{l}_{i,j}$ is the 3-dimensional eigenvector transforming the jth normal coordinate into the mass-weighted Cartesian components of the ith atom. Here $\mathbf{M}_i^{-1/2}$ is the 3×3 diagonal matrix with the same elements of $m_i^{-1/2}$. The $\mathbf{l}$ matrix in eq 24 is directly obtained by diagonalizing the Hessian matrix in the mass-weighted Cartesian coordinates at the transition state, and $\mathbf{f}$ is a 3×3 rotation matrix representing an instantaneous body-fixed frame without overall rotation and translation.

To find the rotation matrix, the authors of ref 17 employed a numerical scheme based on the Newton−Raphson procedure. In this work, however, we have derived such a matrix directly by introducing an Eckart frame[20,21] $\mathbf{f} = (\mathbf{f}_1, \mathbf{f}_2, \mathbf{f}_3)$, such that

$$\mathbf{f} = \mathbf{F}\cdot(\mathbf{F}^{\mathrm{T}}\cdot\mathbf{F})^{-1/2} \quad (25)$$

$$\mathbf{F} = (\mathbf{F}_1, \mathbf{F}_2, \mathbf{F}_3) \quad (26)$$

$$\mathbf{F}_{\alpha} = \sum_{i=1}^{N} c_{i\alpha}m_i^{1/2}\mathbf{x}_i \qquad (\alpha = 1, 2, 3) \quad (27)$$

where $c_{i\alpha}$ is one of the Cartesian components of the i-th atom

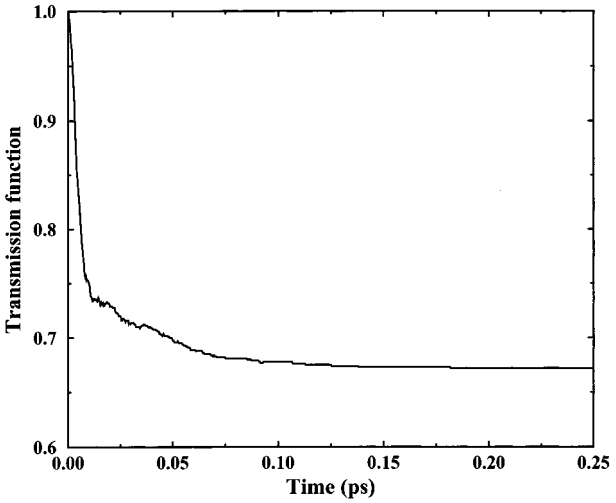

Figure 5. Transmission coefficient κ for the MVK + CPD reaction in water. A total of 2000 trajectories have been averaged, and their initial conditions were obtained at $T = 300$ K.

at the transition state specified in a body fixed frame and $\boldsymbol{x}_i$ is an instantaneous position vector of the i -th atom. Note that $\boldsymbol{F}_i$ are 3-dimensional column vectors. This procedure to find the rotation matrix is quite efficient and easy to implement, since it requires only matrix inversion and diagonalization of the 3 $\times$ 3 Gram matrix ($\boldsymbol{F}^T \cdot \boldsymbol{F}$).[21] Using the current configuration of the system, the Eckart frame defined in eqs 25−27 is calculated once every time the reaction velocity $\dot{\xi}$ is sampled. After the pure Cartesian components are evaluated using eq 24, they are added to the existing velocities obtained by the MD runs described in the previous section to complete the sampling of eq 15.

One can also implement the above algorithm for $P_\xi^c(\Gamma)$ in a different sampling scheme developed by Carter et al.[22] In their method, the dynamic correction factor κ in eq 13 is written as

$$\kappa = \frac{\langle Z_\xi^{-1/2} \dot{\xi}(0) \theta_p[\xi(t_{pl})] \rangle_{\xi,M}}{\langle Z_\xi^{-1/2} \dot{\xi}(0) \theta_p[\dot{\xi}(0)] \rangle_{\xi,M}} \tag{28}$$

where $\langle ... \rangle_{\xi,M}$ denotes averaging over $P_\xi(\mathbf{x}) \cdot P(\mathbf{p}^x|\mathbf{x})$, each of which is defined in eqs 4 and 6, respectively, in ref 22. In this case, one can use only the configurational part sampled by our $P_\xi^c(\Gamma)$ for $P_\xi(\mathbf{x})$ and then generate momentums using $P(\mathbf{p}^x|\mathbf{x})$, which are just Maxwellian distributions in the absence of the molecular constraints.

For the RF calculations, the reactive species surrounded by the periodically replicated 215 water molecules was constrained at $\xi^\ddagger = 2.04$ Å (i.e., the transition state) and equilibrated for 40 ps at $T = 300$ K. Then a total of 2000 RF initial conditions (including both positive and negative reaction coordinate velocities) were generated according to eq 14 for the subsequent recrossing dynamics runs. The resulting transmission function $\kappa(t)$ is plotted with respect to time in Figure 5, showing good convergence toward the plateau region in 0.2 ps. The transmission coefficient κ of the reaction of MVK and CPD in water is found to be 0.67. Thus, based on eq 13, we conclude that the dominant effect of the solvent is a static one, i.e., a reduction in the activation free energy by 2−4 kcal/mol, and that the dynamical recrossing effects are rather minimal by comparison.

V. Concluding Remarks

In this work the free energy barrier and the transmission coefficient for the reaction of MVK + CPD in water has been calculated. For this purpose, an empirical intramolecular PES of this reaction was developed, using the B3LYP/6-31+g* level of ab initio theory. The B3LYP/6-31+g* reaction barrier along the minimum energy path is predicted to be 16.3 kcal/mol in the gas phase. The B3LYP method employed here proved to be a reasonable choice for describing the energetics of the reaction, as was supported by higher levels of ab initio methods such as MP4SDQ and CCSD, although MP2 turns out to perform poorly in this case. The PMF calculations show that the reactive free energy barrier for MVK + CPD in water is 9.5 kcal/mol, which is smaller than the gas phase value by 2.2 kcal/mol. In comparison with the available experimental value, this effect is somewhat underestimated by around 1.6 kcal/mol. Reactive flux calculations find that the transmission coefficient is 0.67, clearly indicating that the dominant solvent effect is a static modification of the activation free energy barrier. The improvement of the underlying modeling techniques used in this paper is the subject of ongoing research in our group and elsewhere.

Acknowledgment. Y.P. thanks S. Jang for the helpful discussions during this study. This research was supported by a grant from the Air Force Office of Scientific Research. We acknowledge generous grants of Silicon Graphics Origin 2000 computer time from the Utah Center for High Performance Computing and the National Center for Supercomputing Applications (MCA941P017N).

Appendix

Denoting the step function $\theta_p[\xi(t)]$ to be $F(\xi,\dot{\xi},t)$, the average value of F with the distribution of eq 15 is given by

$$\langle F \rangle_\pm = \left[\int \mathbf{d}\Gamma\, \delta(\xi - \xi^\ddagger)\, \delta(\dot{\xi}) \exp(-\beta H) \int_0^\infty d\dot{\xi}' \times |\dot{\xi}'| \theta_p(\pm\dot{\xi}') \exp\left(-\frac{1}{2}\beta \dot{\xi}' Z_\xi^{-1} \dot{\xi}'\right) F(\xi,\dot{\xi}',t) \right] \Big/ \left[\int \mathbf{d}\Gamma\, \delta(\xi - \xi^\ddagger) \times \delta(\dot{\xi}) \exp(-\beta H) \int_0^\infty d\dot{\xi}'\, |\dot{\xi}'| \theta_p(\pm\dot{\xi}') \exp\left(-\frac{1}{2}\beta \dot{\xi}' Z_\xi^{-1} \dot{\xi}'\right) \right] \tag{A1}$$

Let us introduce generalized coordinates and their conjugate momentums (q_1, ..., q_{3N-1}, ξ, $p_1 q$, ..., p_{3N-1}^q, p^ξ). Then, using $\mathbf{dp^q}\, d\xi\, dp^\xi = Z_\xi^{-1}\, \mathbf{dp^q}\, d\xi\, d\dot{\xi}$,[16] the change of the integration variables $\mathbf{dp^q}\, d\xi\, dp^\xi$ to $\mathbf{dp^q}\, d\xi\, d\dot{\xi}$ leads to a partition of the kinetic energy term, such that

$$T = T_q + T_\xi \tag{A2}$$

where T_q and T_ξ are the individual kinetic terms depending on p_i^q ($i = 1$, ..., $3N - 1$) and $\dot{\xi}$, respectively. In particular, note that $T_\xi = {}^1/_2 \dot{\xi} Z_\xi^{-1} \dot{\xi}$. (See ref 17 for more details) As a consequence, eq A1 becomes

$$\langle F \rangle_\pm \propto \int \mathbf{dq \cdot dp^q}\, d\xi\, d\dot{\xi}\, Z_\xi^{-1}\, \delta(\xi - \xi^\ddagger)\, \delta(\dot{\xi}) \exp[-\beta(T_q + T_\xi + V)] \int d\dot{\xi}'\, |\dot{\xi}'| \theta_p(\pm\dot{\xi}') \exp\left(-\frac{1}{2}\beta \dot{\xi}' Z_\xi^{-1} \dot{\xi}'\right) F \tag{A3}$$

Integrating eq A3 with respect to $\dot{\xi}$ and changing the order of integration variable $\dot{\xi}'$ gives

$$\langle F\rangle_{\pm} \propto \int \mathbf{dq}\cdot\mathbf{dp}^{\mathbf{q}}\, d\xi\, d\dot{\xi}'\, Z_{\xi}^{-1}\, \delta(\xi - \xi^{\ddagger})|\dot{\xi}'|\theta_{p}(\pm\dot{\xi}') \times \exp\left[-\beta\left(T_q + V + \frac{1}{2}\beta\dot{\xi}' Z_{\xi}^{-1}\dot{\xi}'\right)\right]F$$

$$= \int \mathbf{dq}\cdot\mathbf{dp}^{\mathbf{q}}\, d\xi\, d\dot{\xi}\, Z_{\xi}^{-1}\, \delta(\xi - \xi^{\ddagger})|\dot{\xi}|\theta_{p}(\pm\dot{\xi}) \times \exp(-\beta H)F$$

$$= \int \mathbf{dq}\cdot\mathbf{dp}^{\mathbf{q}} d\xi\, dp^{\xi}\, \delta(\xi - \xi^{\ddagger})|\dot{\xi}|\theta_{p}(\pm\dot{\xi})\exp(-\beta H)F$$

$$= \int \mathbf{d}\Gamma\, \delta(\xi - \xi^{\ddagger})|\dot{\xi}|\theta_{p}(\pm\dot{\xi})\exp(-\beta H)F \qquad \text{(A4)}$$

References and Notes

(1) Rideout, D.; Breslow, R. *J. Am. Chem. Soc*. **1980**, *102*, 7816.
(2) Breslow, R. *Acc. Chem. Res.* **1991**, *24*, 159.
(3) Blake, J. F.; Jorgensen, W. L. *J. Am. Chem. Soc.* **1991**, *113*, 7430.
(4) Jorgensen, W. L.; Blake, J. F.; Lim, D.; Severance, D. *J. Chem. Soc., Faraday Trans.* **1994**, *90*, 1727.
(5) Ruiz-Lopez, M. F.; Assfeld, X.; García, J. I.; Mayoral, J. A.; Salvatella, L. *J. Am. Chem. Soc.* **1993**, *115*, 8780. For a review, see also: Cativiela, C.; García, J. I.; Mayoral, J. A.; Salvatella, L. *Chem. Soc. Rev.* **1996**, 209.
(6) Cramer, C. J.; Truhlar, D. G. *J. Am. Chem. Soc.* **1992**, *114*, 8795.
(7) Chandler, D. *J. Chem. Phys.* **1978**, *68*, 2959.
(8) Minichino, C.; Voth, G. A. *J. Phys. Chem. B* **1997**, *101*, 4544.
(9) Berne, B. J. In *Multiple Time Scales*; Brackbill, J. U., Cohen, B. I., Eds.; Academic: New York, 1985.
(10) Jang, S.; Voth, G. A. *J. Chem. Phys.* **1998**, *107*, 9514.
(11) Frisch, M. J.; Trucks, G. W.; Schlegel, H. B.; Gill, P. M. W.; Johnson, B. G.; Robb, M. A.; Cheeseman, J. R.; Keith, T.; Petersson, G. A.; Montgomery, J. A.; Raghavachari, K.; Al-Laham, M. A.; Zakrzewski, V. G.; Ortiz, J. V.; Foresman, J. B.; Cioslowski, J.; Stefanov, B. B.; Nanayakkara, A.; Challacombe, M.; Peng, C. Y.; Ayala, P. Y.; Chen, W.; Wong, M. W.; Andres, J. L.; Replogle, E. S.; Gomperts, R.; Martin, R. L.; Fox, D. J.; Binkley, J. S.; Defrees, D. J.; Baker, J.; Stewart, J. P.; Head-Gordon, M.; Gonzalez, C.; Pople, J. A. GAUSSIAN 94, Revision E.2; Gaussian, Inc.: Pittsburgh, PA, 1995.
(12) Press: W.; Teukolsky, S. A.; Vetterling, W. T.; Flannery, B. P. *Numerical Recipes*; Cambridge University Press: New York, 1992.
(13) Cornell, W. D.; Cieplak, P.; Bayly, C. I.; Gould, I. R.; Merz, K. M., Jr.; Ferguson, D. M.; Spellmeyer, D. C.; Fox, T.; Caldwell, J. W.; Kollman, P. A. *J. Am. Chem. Soc.* **1995**, *117*, 5179.
(14) Lobaugh, J.; Voth, G. A. *J. Chem. Phys.* **1997**, *106*, 2400.
(15) Bayly, C. I.; Cieplak, P.; Cornell, W. D.; Kollman, P. A. *J. Phys. Chem.* **1993**, *97*, 10269.
(16) den Otter, W. K.; Briels, W. J. *J. Chem. Phys.* **1996**, *106*, 5494.
(17) Wilson, E. B., Jr.; Decius, J. C.; Cross, P. C. *Molecular Vibrations*; Dover Publications: New York, 1955.
(18) Papousek, D.; Aliev, M. R. *Molecular Vibrational−Rotational Spectra*; Elsevier: New York, 1982.
(19) Fukui, K. *Acc. Chem. Res.* **1981**, *14*, 363.
(20) Eckart, C. *Phys. Rev.* **1935**, *47*, 552.
(21) Louck, J. D.; Galbraith, H. W. *Rev. Mod. Phys.* **1976**, *48*, 69.
(22) Carter, E. A.; Ciccotti, G.; Hynes, J. T.; Kapral, R. *Chem. Phys. Lett.* **1989**, *156*, 472.